Detection of ammonia at low concentrations (0.1–2 ppm) with ZnO nanorod-functionalized AlGaN/GaN high electron mobility transistors

Sunwoo JungKwang Hyeon BaikFan RenStephen J. PeartonSoohwan Jang

Citation: Journal of Vacuum Science & Technology B, Nanotechnology and Microelectronics: Materials, Processing, Measurement, and Phenomena **35**, 042201 (2017); doi: 10.1116/1.4989370

View online: http://dx.doi.org/10.1116/1.4989370

View Table of Contents: http://avs.scitation.org/toc/jvb/35/4

Published by the American Vacuum Society

Detection of ammonia at low concentrations (0.1–2 ppm) with ZnO nanorod-functionalized AlGaN/GaN high electron mobility transistors

Sunwoo Jung
Department of Chemical Engineering, Dankook University, Yongin 16890, South Korea

Kwang Hyeon Baik
School of Materials Science and Engineering, Hongik University, Jochiwon, Sejong 30016, South Korea

Fan Ren
Department of Chemical Engineering, University of Florida, Gainesville, Florida 32611

Stephen J. Pearton
Department of Materials Science and Engineering, University of Florida, Gainesville, Florida 32611

Soohwan Jang[a)]
Department of Chemical Engineering, Dankook University, Yongin 16890, South Korea

(Received 29 March 2017; accepted 8 June 2017; published 21 June 2017)

AlGaN/GaN high electron mobility transistors with ZnO nanorod functionalized gates were used for detecting NH_3 in the concentration range of 0.1–2 ppm balanced with air at ambient temperatures from 25 to 300 °C. A decrease in the high electron mobility transistor drain current was observed for exposure to the NH_3-containing ambients, indicating an increase in negative charge at the heterointerface. The detection sensitivity increased monotonically with ammonia concentration at all temperatures, from 0.28% (25 °C) and 3.17% (300 °C) for 0.1 ppm to 1.32% (25 °C) and 13.73% (300 °C) for 2 ppm for a drain–source voltage of 1 V. The latter condition is attractive for low power consumption. The sensitivity was also a function of applied voltage and was generally higher in the linear region of the current–voltage characteristic of the transistor. The activation energy of the sensitivity was 0.09 eV, and the sensors showed no response to O_2 (100%), CO_2 (10%), CO (0.1%), CH_4 (4%), and NO_2 (0.05%) under the same detection conditions as used for the NH_3. The response was less than 1 s, and recovery times were of order ~53 s at 25 °C. [http://dx.doi.org/10.1116/1.4989370]

I. INTRODUCTION

Detection of ammonia at low concentrations is a necessary capability for monitoring releases in the environment from refrigeration and agricultural (fertilizer and livestock) systems as well as in the automotive and chemical industries.[1–11] In addition, the emission of nitrogen oxides, or NOx, is a global pollution issue resulting in acid rain and formation of ground-level ozone that produces smog in urban areas. Various technologies have been developed to control emission of nitrogen oxides, with the most common being the selective catalytic reduction (SCR) process.[2,4–7] This works by reacting the NOx with gaseous ammonia over a vanadium catalyst to produce elemental nitrogen and water vapor and it has been widely employed to reduce emissions from flue gases from boilers, refinery off-gas combustion, gas and diesel engines, and gas turbines in the power industry and chemical process gas streams.[4–7,12] NOx removal rates in excess of 95% can be achieved with the SCR process.[10] Reliable NH_3 sensors are therefore needed to monitor leaks during the NH_3 injection to reduce NOx emissions of diesel engines and industrial plants.[2,10,13]

There have been many reports on the development of ammonia sensors, including metal oxide-based thin films and nanostructures of pure or metal-doped ZnO, SnO_2, In_2O_3, and WO_3 (Refs. 11–27) as well as functionalized carbon nanotubes. These generally exhibit sensitivities in the range of 2–90 for 1–30 ppm of NH_3 in the temperature range 25–300 °C.[1,10] AlGaN/GaN high electron mobility transistors (HEMTs)[28–35] are attractive candidates for such applications because of their high temperature stability, corrosion resistance, and chemical stability compared to silicon, which gives them advantages for automotive exhaust gas sensors.[23]

In this work, we have studied the concentration and temperature dependence of NH_3 detection sensitivities of ZnO nanorod functionalized AlGaN/GaN HEMTs in air backgrounds, ranging from 25 to 300 °C. The use of the HEMT platform allows for the amplification effect of a transistor, while the ZnO nanorods were prepared with a sol–gel method to lower the cost of the metal oxide growth.

II. EXPERIMENT

HEMT layer structures were grown on *c*-plane sapphire by metal organic chemical vapor deposition. The layer structure included an initial 2 μm thick undoped GaN buffer followed by a 25 nm thick unintentionally doped $Al_{0.25}Ga_{0.75}N$ layer. Sensor fabrication began with Ti/Al/Ni/Au (25/125/45/100 nm) metal deposition to form 50 × 50 μm Ohmic contact pads separated by a gap of 20 μm with the standard lift-off of e-beam evaporated Ti/Al/Ni/Au-based metallization, and the samples were subsequently annealed at 850 °C for

a)Electronic mail: jangmountain@dankook.ac.kr

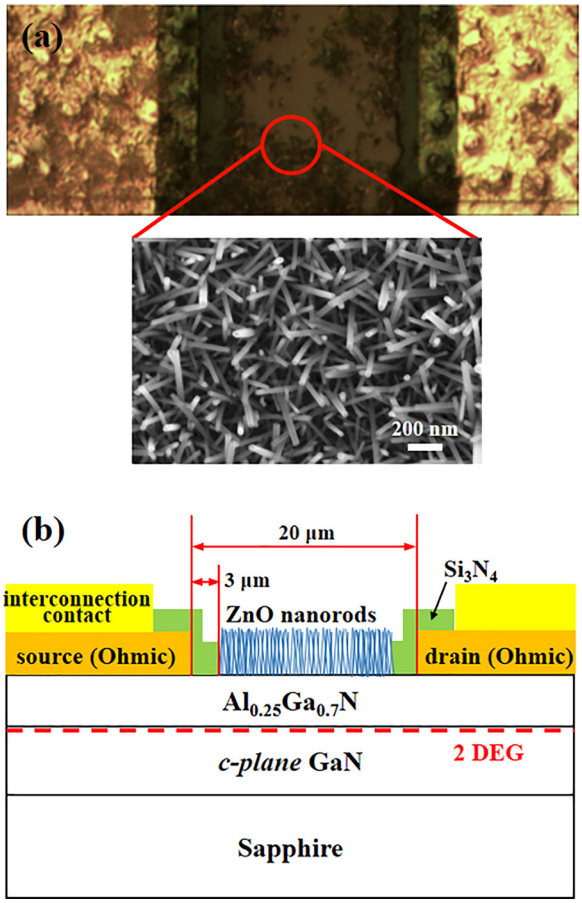

FIG. 1. (Color online) (a) Top-view optical microscope image of ZnO-functionalized AlGaN/GaN HEMT sensor and SEM image of ZnO nanorods grown on the gate region. (b) Cross-sectional schematic image of ZnO nanorod-AlGaN/GaN HEM.

45 s under a flowing N_2 ambient in a Heatpulse 610T system.[31] Multiple energy and dose nitrogen ion implantation was used for the device isolation and photoresist (AZ1045) was used as the mask to define the active region of the devices. Interconnection contacts were formed by lift-off of e-beam deposited Ti/Au (20/100 nm). A 250 nm thick plasma-enhanced chemical vapor deposited silicon nitride layer was used to passivate the source/drain regions.[31] The gate and contact pad regions were defined using conventional photolithography and buffered oxide etchant for the subsequent ZnO nanorod growth on the AlGaN surface and electrical probing of the devices.

The gate area of the sensors was functionalized with ZnO nanorods for NH_3 sensing.[29,30,32] The ZnO nanorod growth was started with ZnO nanocrystal seed preparation. ZnO nanocrystal seed solution was mixed by slowly adding 30 mM NaOH (Sigma–Aldrich) in methanol to a 10 mM zinc acetate dihydrate [$Zn(O_2CCH_3)_2{\cdot}2H_2O$, Sigma–Aldrich] solution at 60 °C over a 2 h period. The ZnO nanocrystal seed solution was spun on the HEMT, and then, the sample was heated on a hot plate at 300 °C for 30 min in an air ambient. The nanocrystalline seed coated sensor chips were then immersed in an aqueous mixture of 20 mM zinc nitrate hexahydrate [$Zn(NO_3)_2{\cdot}6H_2O$, Sigma–Aldrich] and 20 mM hexamethylenetetramine ($C_6H_{12}N_4$, Sigma–Aldrich) and put in the oven at ~94 °C for 3 h for the ZnO nanorod growth.[20] After the nanorod growth, the device was removed from the solution, thoroughly rinsed with deionized water to remove any residual salts, and dried with nitrogen gas. Photoresist was used to pattern the gate area, and dilute 1 HCl:10 H_2O solution was used to etch off the ZnO nanorods around the gate and contact pad area.[29,30] An optical microscope image and schematic structure of the fabricated ZnO-functionalized AlGaN/GaN HEMT sensor is shown in Fig. 1. Also, a top-view scanning electron microscope (SEM) image of ZnO nanorods grown on the gate area of AlGaN/GaN HEMT is presented in Fig. 1(a).

The completed diodes were exposed to controlled concentrations of NH_3 balanced with synthetic air in a test chamber in which mass flow controllers controlled the gas flow rate and injection time. The sensors were mounted on a probe stage in the chamber with electrical feed-throughs connected to an HP4155C parameter analyzer.[36–38] The devices were exposed to NH_3 concentrations of 0.1–2 ppm at temperatures from 25 to 300 °C.

III. RESULTS AND DISCUSSION

Figure 2(a) shows that the sensors were completely selective at 25 °C for 2 ppm NH_3 over O_2 (100%), CO_2 (10%), CO (0.1%), CH_4 (4%), and NO_2 (0.05%) under the same detection conditions as used for the NH_3. The concentrations of the other gases were chosen in the range of U.S. health exposure limits set by the National Institute for Occupational Safety and Health.[39,40] The exposure time to each of these gases was for 20 s each, and the source–drain voltage on the HEMT was 4 V. The current response for 2 ppm NH_3 at 25 °C in a magnified time scale is shown in Fig. 2(b).

Figure 3 shows the drain current–voltage (I–V) characteristics of the HEMT sensor at four different temperatures (25, 100, 200, and 300 °C) in either air or 2 ppm NH_3. Note that the drain current decreases in all cases, which is the opposite to what we observed with the detection of reducing gases with HEMT sensors. In that case, the detection mechanism involves an increase in positive charge at the heterointerface that creates the two-dimensional electron gas (2DEG) used as the transistor channel.[31,36–38] For example, a hydrogen sensor employs a catalytic Schottky gate metal, platinum, in the gate region. The 2DEG channel is very sensitive to changes in AlGaN surface charge. When a HEMT of this type is exposed to hydrogen gas, hydrogen molecules are adsorbed on the active sites of the platinum before being decomposed into atoms. Then, the dissociated hydrogen atoms diffuse into the AlGaN interface to form effective positive gate surface charges, thereby enhancing the 2DEG channel and increasing drain current.[31,36–38] In effect, the drain current response to hydrogen is amplified through the 2DEG of AlGaN/GaN heterostructure.

The role of the ZnO nanorods can be described as follows: In the present case of NH_3 detection, the 2DEG current decreases upon exposure to the gas, suggesting that there is an increase in negative charge at the heterointerface. The

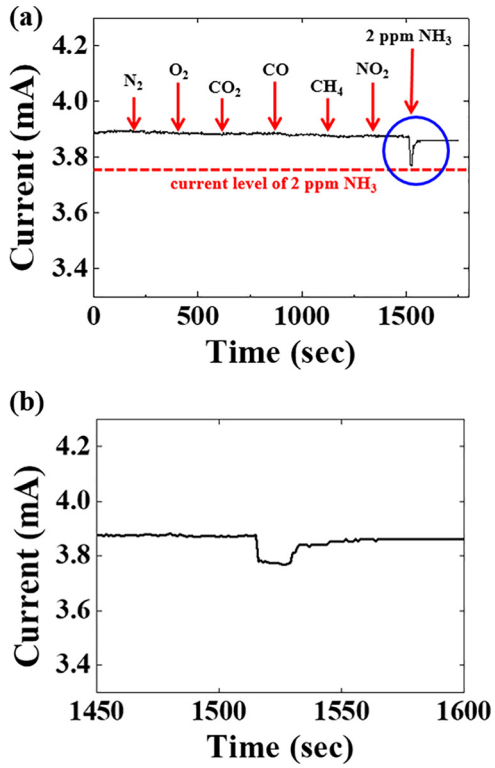

FIG. 2. (Color online) (a) Response of sensor to 20 s sequential exposures of O_2 (100%), CO_2 (10%), CO (0.1%), CH_4 (4%), NO_2 (0.05%), and NH_3 (2 ppm) at 25 °C. The drain–source voltage (V_{DS}) was fixed at 4 V. (b) The zoomed plot of (a) in a magnified time scale for 2 ppm NH_3 at 25 °C.

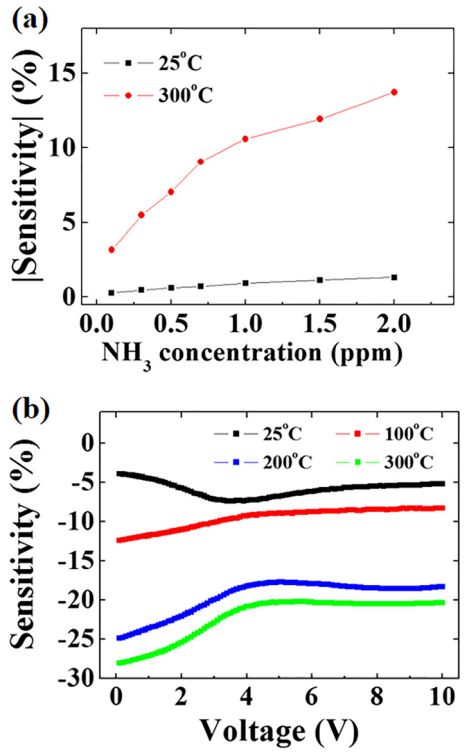

FIG. 4. (Color online) (a) Absolute sensitivity of sensors as a function of NH_3 concentration for either 25 or 300 °C at V_{DS} of 1 V, and (b) sensitivity as a function of V_{DS} at four different temperatures (25, 100, 200, or 300 °C) for continuous 2 ppm NH_3 exposure.

mechanism of ammonia reacting with the ZnO nanorods may involve adsorption of oxygen that is reduced by electrons in the n-type ZnO,[1] leading to the reaction $2NH_3 + 3O^-_{ads} \leftrightarrow 3H_2O + N_2 + 3e^-$. The ZnO nanorods exhibit n-type conductivity related to oxygen vacancies and therefore can significantly enhance oxygen molecular adsorption.[1] The oxygen species react with the ammonia to return more electrons to the ZnO surface, resulting in an abrupt change in the conductivity of 2DEG channel of the HEMT sensor and enhancing the gas-sensing properties of the nanorod-functionalized HEMT. This is opposite to the trend with the detection of hydrogen, where the current increases and also when similar sensors are employed at temperatures of 150 °C and higher to detect CO.[30] In that case, the chemisorbed oxygen on the oxide surface reacts with CO, forming CO_2, and releasing electrons to the oxide surface. Those electrons make the oxide surface more negative and induce additional positive charges on the AlGaN surface in the gate area as well as extra electrons in the 2DEG channel.[41,42] All of this data show that charge transfer through the ZnO nanorods upon adsorption of different gases over a range of temperatures is effective when they are present in the gate region of HEMTs.

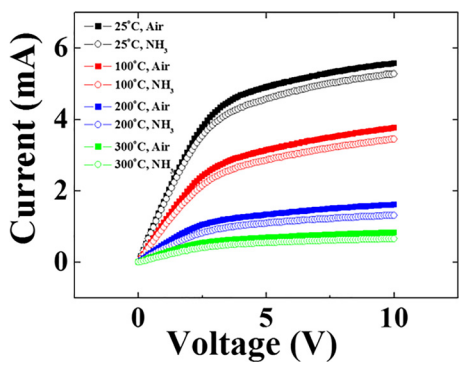

FIG. 3. (Color online) HEMT sensor drain–source current characteristics measured in air or 2 ppm NH_3 at 25, 100, 200, and 300 °C.

The sensitivity of the sensors is defined as $(I_{NH_3} - I_{air}/I_{air}) \times 100\%$, where I_{NH_3} is the current under the various concentrations of ammonia and I_{air} is the current under an air ambient. As shown in Fig. 4(a), the absolute detection sensitivity increased monotonically with ammonia concentration at all temperatures, from 0.28% (25 °C) and 3.17% (300 °C) for 0.1 ppm to 1.32% (25 °C) and 13.73% (300 °C) for 2 ppm for a drain–source voltage of 1 V. The latter condition is attractive for low power consumption and is in the linear region of the HEMT I–V plot. The sensitivity was also a function of applied voltage and was generally higher at lower biases where the HEMT shows linear I–V characteristics (Fig. 3), as shown in Fig. 4(b). Thus, the HEMT provides a wide voltage operation range, and the choice of bias can be chosen based on power consumption requirements.

The response and recovery of the sensors is important for achieving precise control of antipollution systems.[33] Response time was defined as the time required to reach

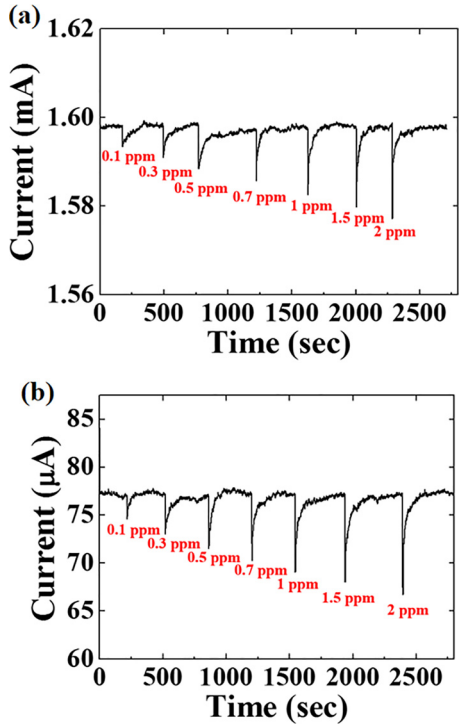

FIG. 5. (Color online) Time response of sensors to 5 s exposures of 0.1–2 ppm NH_3, followed in each case by a return to refreshing air with V_{DS} of 1 V at (a) 25 and (b) 300 °C.

90% of saturated current after 2 ppm ammonia exposure, and recovery time was defined as the time required to reach 10% of the saturated current after refreshing air exposure. Response times for all concentrations of ammonia exposures were 1 s, which was the unit measurement time for both 25 and 300 °C, as shown in Fig. 5. The recovery times were faster at higher temperature. The recovery times for 2 ppm ammonia were 53 and 40 s for 25 and 300 °C, respectively.

Figure 6 shows an Arrhenius plot of sensitivity, leading to an activation energy of 0.09 eV for ammonia sensing with the ZnO nanorod-functionalized HEMT. This is the energy of the rate-limiting step in the formation of a charge depletion layer on the surface of the ZnO due to electron trapping on adsorbed oxygen species and the transfer of the negative charge to the AlGaN surface from the reaction discussed earlier.[1,10,11]

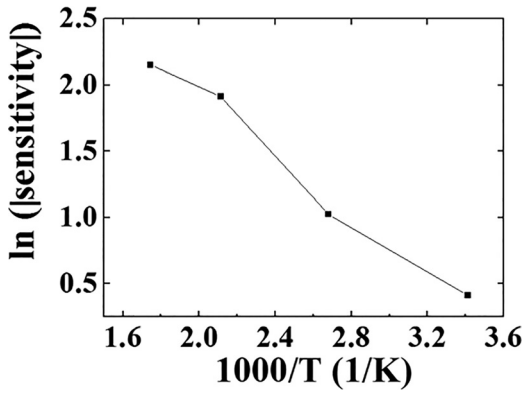

FIG. 6. Arrhenius plot of sensitivity to detection of 2 ppm NH_3.

IV. SUMMARY AND CONCLUSIONS

ZnO-nanorod-functionalized AlGaN/GaN HEMT sensors are shown to be capable of ammonia detection at low concentrations (0.1–2 ppm) at temperatures in the range 25–300 °C. The sensors are completely selective to the presence of other common gases such as O_2, CO_2, CO, CH_4, and NO_2. The drain current in the HEMTs decreases upon exposure to ammonia-containing ambients, indicating that negative charge is produced at the heterointerface. The chemical and temperature stability of the AlGaN/GaN suggests that these sensors are attractive candidates for applications like automobile exhaust sensing.

ACKNOWLEDGMENTS

This research was supported by the Basic Science Research Program through the National Research Foundation of Korea (NRF) funded by the Ministry of Education (2017R1D1A3B03035420, 2015R1D1A1A01058663), and Nano Material Technology Development Program through the National Research Foundation of Korea (NRF) funded by the Ministry of Science, ICT and Future Planning (2015M3A7B7045185). The work at UF was partially supported by HDTRA1-17-1-001.

[1]C. S. Rout, M. Hegde, A. Govindaraj, and C. N. R. Rao, Nanotechnology **18**, 205504 (2007).
[2]B. Timmer, W. Olthuis, and A. Berg, Sens. Actuators, B **107**, 666 (2005).
[3]M. Aslam, V. A. Chaudhary, I. S. Mulla, S. R. Sainkar, A. B. Mandale, A. A. Belhekar, and K. Vijayamohanan, Sens. Actuators, A **75**, 162 (1999).
[4]M. S. Wagh, G. H. Jain, D. R. Patil, S. A. Patil, and L. A. Patil, Sens. Actuators, B **115**, 128 (2006).
[5]Y. Wang, X. Wu, Q. Su, Y. Li, and Z. Zhou, Solid-State Electron. **45**, 347 (2001).
[6]P. Guo and H. Pan, Sens. Actuators, B **114**, 762 (2006).
[7]E. Bekyarova, M. Davis, T. Burch, M. E. Itkis, B. Zhao, S. Sushine, and R. C. Haddon, J. Phys. Chem. B **108**, 19717 (2004).
[8]N. H. Quang, M. V. Trinh, B. Lee, and J. Huh, Sens. Actuators, B **113**, 341 (2006).
[9]F. V. Paez, A. H. Romero, E. M. Sandoval, L. M. Martinez, H. Terrones, and M. Terrones, Chem. Phys. Lett. **386**, 137 (2004).
[10]C. S. Rout, S. H. Krishna, S. R. C. Vivekchand, A. Govindaraj, and C. N. R. Rao, Chem. Phys. Lett. **418**, 586 (2006).
[11]C. S. Rout, A. Govindaraj, and C. N. R. Rao, J. Mater. Chem. **16**, 3936 (2006).
[12]I. Jiménez, J. Arbiol, A. Cornet, and J. R. Morante, IEEE Sens. J. **2**, 329 (2002).
[13]B. Marquis and J. Vetelino, Sens. Actuators, B **77**, 100 (2001).
[14]D. Zhang, C. Jiang, and Y. Sun, J. Alloys Compd. **698**, 476 (2017).
[15]S. Han, X. Zhuang, Y. Jiang, X. Yang, L. Li, and J. Yu, Sens. Actuators, B **243**, 1248 (2017).
[16]F. Rigoni, S. Tognolini, P. Borghetti, G. Drera, S. Pagliara, A. Goldoni, and L. Sangaletti, Procedia Eng. **87**, 716 (2014).
[17]R. H. Vignesh, K. V. Sankar, S. Amaresh, Y. S. Lee, and R. K. Selvan, Sens. Actuators, B **220**, 50 (2015).
[18]J. Samà, S. Barth, G. Domènech-Gil, J. D. Prades, N. López, O. Casals, I. Gràcia, C. Cané, and A. Romano-Rodríguez, Sens. Actuators, B **232**, 402 (2016).
[19]J. M. Tulliani, A. Cavalieri, S. Musso, E. Sardella, and F. Geobaldo, Sens. Actuators, B **152**, 144 (2011).
[20]A. G. Bannov, J. Prášek, O. Jašek, A. A. Shibaev, and L. Zajíčková, Procedia Eng. **168**, 231 (2016).
[21]B. Chatterjee and A. Bandyopadhyay, Environ. Qual. Manage. **26**, 89 (2016).
[22]M. Gautam and A. H. Jayatissa, J. Appl. Phys. **111**, 094317 (2012).
[23]D. A. Burgard, T. R. Dalton, G. A. Bishop, J. R. Starkey, and D. H. Stedman, Rev. Sci. Instrum. **77**, 014101 (2006).

[24]V. B. Raj, A. T. Nimal, Y. Parmar, M. U. Sharma, and V. Gupta, Sens. Actuators, B **166**, 576 (2012).
[25]G. S. T. Rao and D. T. Rao, Sens. Actuators, B **55**, 166 (1999).
[26]Y. L. Tang, Z. J. Li, J. Y. Ma, Y. J. Guo, Y. Q. Fu, and X. T. Zu, Sens. Actuators, B **201**, 114 (2014).
[27]X. Wang, J. Zhang, and Z. Zhu, Appl. Surf. Sci. **252**, 2404 (2006).
[28]X. Jia, D. Chen, L. Bin, H. Lu, R. Zhang, and Y. Zheng, Sci. Rep. **6**, 27728 (2016).
[29]S. C. Hung, W. Y. Woon, F. Ren, and S. J. Pearton, Appl. Phys. Lett. **103**, 083506 (2013).
[30]C. F. Lo, Y. Xi, L. Liu, S. J. Pearton, S. Doré, C. H. Hsu, A. M. Dabiran, P. P. Chow, and F. Ren, Sens. Actuators, B **176**, 708 (2013).
[31]B. S. Kang, H. T. Wang, F. Ren, and S. J. Pearton, J. Appl. Phys. **104**, 031101 (2008).
[32]B. H. Chu *et al.*, Appl. Phys. Lett. **93**, 042114 (2008).
[33]Y. Halfaya, C. Bishop, A. Soltani, S. Sundaram, V. Aubry, P. L. Voss, J. P. Salvestrini, and A. Ougazzaden, Sensors **16**, 273 (2016).
[34]H. I. Chen, Y. J. Liu, C. C. Huang, C. S. Hsu, C. F. Chang, and W. C. Liu, Sens. Actuators, B **155**, 347 (2011).
[35]H. I. Chen, C. S. Hsu, C. C. Huang, C. F. Chang, P. C. Chou, and W. C. Liu, IEEE Electron Device Lett. **33**, 612 (2012).
[36]S. Jang, J. Kim, and K. H. Baik, J. Electrochem. Soc. **163**, B456 (2016).
[37]K. H. Baik, J. Kim, and S. Jang, ECS Trans. **72**, 23 (2016).
[38]S. Jang, P. Son, J. Kim, S. Lee, and K. H. Baik, Sens. Actuators, B **222**, 43 (2016).
[39]S. Jung, K. H. Baik, F. Ren, S. J. Pearton, and S. Jang, IEEE Electron Device Lett. **38**, 657 (2017).
[40]J. Hong, S. Lee, J. Seo, S. Pyo, J. Kim, and T. Lee, ACS Appl. Mater. Interfaces **7**, 3554 (2015).
[41]S. C. Hung, C. W. Chen, C. Y. Shieh, G. C. Chi, R. Fan, and S. J. Pearton, Appl. Phys. Lett. **98**, 223504 (2011).
[42]C. F. Lo, B. Y. Chu, S. J. Pearton, A. Dabiran, P. Chow, S. Dore, S. C. Hung, C. W. Chen, and F. Ren, Appl. Phys. Lett. **99**, 142107 (2011).